

Review

# Advances in Stimuli-Responsive Soft Robots with Integrated Hybrid Materials

Hyegyo Son <sup>1</sup> and ChangKyu Yoon <sup>1,2,\*</sup> 

<sup>1</sup> Department of Mechanical Systems Engineering, Sookmyung Women's University, Seoul 04310, Korea; shg10@sookmyung.ac.kr

<sup>2</sup> Institute of Advanced Materials and Systems, Sookmyung Women's University, Seoul 04310, Korea

\* Correspondence: ckyoon@sookmyung.ac.kr

Received: 26 September 2020; Accepted: 11 November 2020; Published: 14 November 2020



**Abstract:** Hybrid stimuli-responsive soft robots have been extensively developed by incorporating multi-functional materials, such as carbon-based nanoparticles, nanowires, low-dimensional materials, and liquid crystals. In addition to the general functions of conventional soft robots, hybrid stimuli-responsive soft robots have displayed significantly advanced multi-mechanical, electrical, or/and optical properties accompanied with smart shape transformation in response to external stimuli, such as heat, light, and even biomaterials. This review surveys the current enhanced scientific methods to synthesize the integration of multi-functional materials within stimuli-responsive soft robots. Furthermore, this review focuses on the applications of hybrid stimuli-responsive soft robots in the forms of actuators and sensors that display multi-responsive and highly sensitive properties. Finally, it highlights the current challenges of stimuli-responsive soft robots and suggests perspectives on future directions for achieving intelligent hybrid stimuli-responsive soft robots applicable in real environments.

**Keywords:** responsive materials; hybrid actuators; intelligent systems; 2DLMs; soft robotics

## 1. Introduction

An extensive comprehensive discussion of stimuli-responsive soft robots has been reviewed in the forms of flexible electronics, sensors, biomedical tools, optics, and actuators [1–7]. In general, stimuli-responsive soft robots are mainly composed of polymer, hydrogel, or hybrid of them both, which provide significantly larger swelling than their dehydrated weight due to their inherent porous nature [8]. Thus, various stimuli-responsive soft robots have displayed smart shape transformation via the reversible swelling–deswelling process in aqueous environments when triggered by external cues, such as heat, pH, light, and even sequence of DNAs [2]. When creating the shape-changing soft robots, the development of engineered stimuli-responsive materials is an indispensable first point to be considered. One of the elegant approaches to incur shape-changing is to adjust the physiochemical properties of the swelling–deswelling process by controlling the crosslinking density [8]. Accordingly, this design of stimuli-responsive materials (e.g., hydrogel-network system) allows the adjustment of a lower critical solution temperature (LCST) to display unique physiochemical property changes inside a material system in specified environments [9]. Along with these unique properties of stimuli-responsive soft robots, the swelling (below the LCST)–deswelling (above the LCST) processes can exhibit a considerable shape transformation of soft machines in specified aqueous environments. For example, *N*-isopropylacrylamide (NIPAM), one of the primarily utilized thermally responsive materials, has shown that LCST-based properties change between 32 °C and 36 °C, and they exhibit smart shape-changing near the physiological temperature [9–11], which can be potentially utilized as smart healthcare soft robots for precise and non-invasive drug delivery or biopsy [10,11]. The NIPAM-based hydrogels have been extensively utilized

for shape-changeable thermally responsive soft robots due to the easily accessible heat source [12–15]. These thermally-responsive NIPAM-based soft robots are of continuing interest as they provide intelligent perspectives on the ease of shape transformation. From a different perspective of shape transformation, the shape-changing mechanisms of stimuli-responsive soft robots are mainly based on inhomogeneous configurations, such as bilayer, bi-strip, heterogeneous monolayer, or helical geometries [2,16]. In particular, bilayering is one of the primary techniques to build shape-changing soft robots [2]. The bilayer, which is composed of stimuli-responsive and stimuli-non-responsive layers, displays a heterogeneous response between layers when exposed to stimuli, which enables it to fold, bend, or roll itself into complex three-dimensional (3D) structures similar to a paper origami. Furthermore, the principles of shape transformation are dependent on the types of stimuli-responsive materials and the stimuli sources, as well as on the methodologies used to construct those systems. To develop shape-changing soft robots, a variety of structuring or patterning techniques have been proposed, including photolithography, 3D printing, and soft molding [17–19]. Recently, using these techniques, stimuli-responsive hydrogels combined with nanoparticles or/and low dimensional materials have been developed to realize multi-functional, multi-responsive, and highly sensitive soft machines.

A variety of comprehensive reviews that focus on stimuli-responsive hydrogels and their applications have been proposed [4–6,20–23]. In addition, shape changeable stimuli-responsive machines have been broadly discussed for more comprehensive analysis of soft robotics [1–3,7,24–26]. More recently, reviews of integrated hybrid stimuli-responsive soft robots for multi-scale systems have been actively discussed [18,19,21,23–28] but most of them have partially discussed the hybrid stimuli-responsive soft robots combined with multi-functional materials. In this regard, this review primarily aims to provide the recent progress of hybrid stimuli-responsive soft robots (e.g., actuators and sensors) combined with functional materials, such as carbon-based nanoparticles, nanowires, low-dimensional materials, and liquid crystals. In the first part, we summarize the current developments of various synthesizing strategies for integrating these functional materials with stimuli-responsive soft machines. In addition, we present several applications of hybrid stimuli-responsive soft machines, such as multi-responsive, multi-functional, and highly sensitive actuators and sensors. Afterwards, we provide our perspectives on the recent developments of stimuli-responsive soft robots with integrated hybrid materials and suggest challenges and possible new areas of interest.

## 2. Hybrid Materials Selection

The hybridization of stimuli-responsive materials with additives such as nanoparticles, low-dimensional materials, and liquid crystalline materials has shown new directions for exploiting advanced stimuli-responsive shape-changing soft machines. In particular, these additives have shown new ways to reversibly deform material properties with successive shape transformations of soft machines when exposed to external cues, such as heat and light. Thus, this section reviews several types of additives and their properties that trigger smart shape-changing stimuli-responsive soft machines. In particular, the description mainly covers the roles of nanowires, carbon nanotubes (CNTs), carbon-based graphene, graphene oxides (GOs), molybdenum disulfide ( $\text{MoS}_2$ ), liquid crystals, and hybrids to create multi-functional, multi-responsive, and highly sensitive shape changeable soft machines.

### 2.1. Nanowires-Stimuli-Responsive Composite Gels

To enhance the electrothermal and optical properties, various nanowire additives have been extensively adapted to manufacture stimuli-responsive shape-changing soft machines [29–37]. The nanowires can absorb a certain wavelength of light, which transfers to thermal energy, allowing the shape transformation of thermally responsive soft machines. Based on the selective optothermal properties of the nanowire additives, Lee et al. presented a single photomechanical nanowire 3D actuator in nanoscales by azobenzene nanowire photoisomerization (Figure 1A) [29]. In a brief description, they suggested the meniscus-guided method to fabricate the azobenzene vertically for creating an untethered photomechanical nanowire tweezer composed of an azobenzene nanowire and

polystyrene (PS) nanowire. In particular, the asymmetric light response properties of azobenzene (light responsive) and PS-nanowire (non-light responsive) result in spontaneous bending when exposed to UV light. The outstanding feature of this tweezing actuator is that the actuation can selectively respond to only certain ranges of wavelengths, such as visible light based on the plasmonic effect. Furthermore, Wu et al. proposed a new way to incur shape changing via sliding networks of copper (Cu) nanowires during the voltage on/off process (Figure 1B) [30]. The Cu nanowire embedded acrylic elastomeric film actuator was deformed up to an area strain of 200% when 4.8 kV was applied, and Cu nanowires could slide across each other while maintaining electrical function with feasible reversibility of operation. They also reported that the transmittance was increased by 4.5 times from 13% to 58%, which was higher than that of conventional carbon nanotube electrodes.

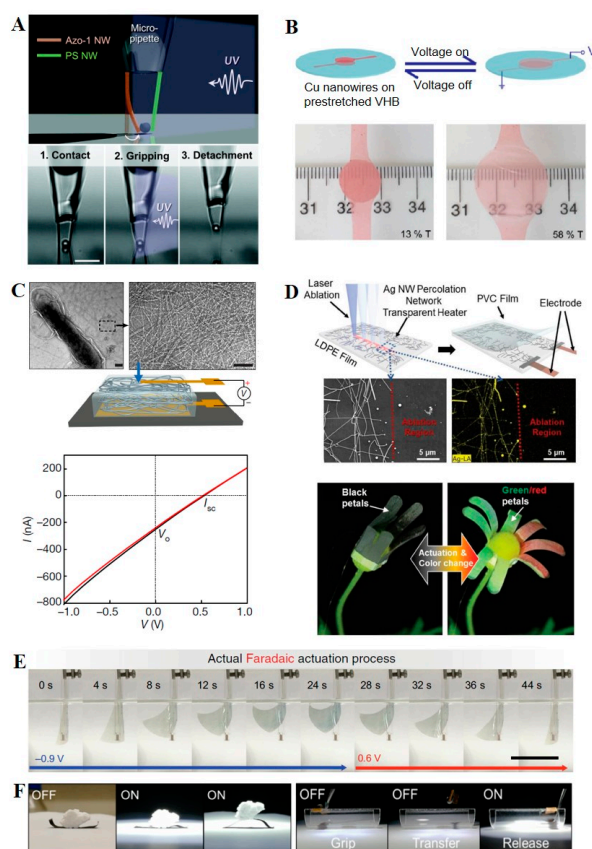


**Figure 1.** (A) Photomechanical nanowire tweezer composed of an azobenzene nanowire and polystyrene (PS) nanowire. Reproduced with permission [29]. Adapted with permission under the terms of the Creative Commons Attribution Non Commercial License 3.0, copyright 2015, the authors. (B) Shape-changing acrylic elastomer and copper (Cu) composite film via sliding networks of copper (Cu) nanowires during the voltage on/off process. Reproduced with permission [30], copyright 2013, American Chemical Society. (C) Electric power generator composed of protein nanowires and a gold (Au) electrode thin film on a glass substrate. Reproduced with permission [31], copyright 2020, Nature Publishing Group. (D) Biomimetic color-shifting anisotropic soft actuator composed of low-density polyethylene (LDPE) and polyvinyl chloride (PVC) bilayer films with silver nanowire (Ag NWs) percolation networks. Reproduced with permission [32], copyright 2018, Wiley-VCH. (E) Color/shape dual responsive actuator composed of tungsten oxide ( $W_{18}O_{49}$ ) and silver (Ag) nanowires bilayer networks. Reproduced with permission [33], adapted with permission under the terms of the Creative Commons Attribution Non Commercial License 4.0, copyright 2018, the authors. (F) Multi-stimuli-responsive soft gripper using vanadium dioxide ( $VO_2$ ) nanowires and carbon nanotube composites. Reproduced with permission [34], adapted with permission under the terms of the Creative Commons Attribution Non Commercial License 4.0, copyright 2020, the authors.

Innovative trials have been conducted using living additives directly combined with metallic or ceramic materials, which exploit new concepts of biological actuators or electric generators. Liu et al. proposed an enhanced electric power generator using protein nanowires (Figure 1C) [31]. They developed an electric generator composed of nanoscale proteins and a gold (Au) electrode thin film on a glass substrate. The biological sensors showed the self-maintained moisture gradient driven energy harvesting within the film when exposed to humidity in the air. One significant feature of this sensor is that the current–voltage curve was approximately linear during power output due to the mass protein nanowires. Moreover, they verified that the electric generator could produce a continuous current for at least 20 h and could self-recharge.

Inspired by the shape transformation of biological systems, biomimetic shape-changing hybrid soft machines combined with nanowire additives have also been extensively developed. Recently, Kim et al. developed an advanced biomimetic color-shifting anisotropic soft actuator (CASA) composed of low-density polyethylene (LDPE) and polyvinyl chloride (PVC) bilayer films with silver nanowire (Ag NWs) percolation networks (Figure 1D) [32]. They adapted an UV laser ablation method to fabricate thin film structures to achieve a smart biomimetic actuator and an optically color switching function. In particular, they fabricated a flower-shaped machine composed of eight serially connected domains as petals that displayed reversible bending and flattening when the voltage ( $V_{DC}$ ) was applied. They further demonstrated that it achieved a significantly large curvature, up to  $2.5\text{ cm}^{-1}$ , and a notable performance reliability of over 10,000 operating cycles.

Furthermore, Li et al. proposed a color/shape dual responsive actuator composed of tungsten oxide ( $W_{18}O_{49}$ ) and silver (Ag) nanowire bilayer networks on ultrathin poly(3,4-ethylenedioxythiophene)-poly(styrenesulfonate) (PEDOT:PSS) (Figure 1E) [33]. This multi-responsive actuator displayed a reversible operation, which responded fast ( $<5\text{ s}$ ), and highly synchronized flexible actuators driven by the pseudo-capacitance-based reversible lattice contraction/recovery process of  $W_{18}O_{49}$  nanowires. Chen et al. proposed a multi-stimuli-responsive soft robot using a vanadium dioxide ( $VO_2$ ) nanowire (Figure 1F) [34]. In particular, they designed an insect-scale gripper consisting of super aligned  $VO_2$  nanowires and a carbon nanotube (CNT) bimorph composite film that was actuated by various stimuli such as heat, light, and electricity. They demonstrated that the photothermal-driven gripper could lift a target within 6 s and hold a copper strip (50 times heavier than a gripper) under light illumination. A variety of these nanowires have been extensively adapted to create highly sensitive and multi-functional stimuli-responsive shape-changing soft machines due to their excellent electrothermal and optical properties.

## 2.2. Carbon Nanotubes (CNT)-Stimuli-Responsive Composite Gels

Carbon nanotubes (CNTs) have been utilized in soft robotics due to their excellent optical, thermal, electrical, and mechanical properties [38–47]. CNTs have displayed highly enhanced electrical-to-thermal or optical-to-thermal energy transmissions, triggering the smart shape deformation of stimuli-responsive soft robots. For example, Zhang et al. proposed a highly versatile photoactuator composed of single-walled carbon nanotube (SWCNT) and polycarbonate (PC) polymer bilayers (Figure 2A) [43]. They utilized high light-absorbing SWCNTs that could convert photon energy to heat, which diffused to the PC layer, resulting in shape deformation of a bilayer sheet. They demonstrated that the SWCNT/PC bilayers can curl and flatten reversibly according to the light on/off processes. Specifically, they observed a large bending deflection of SWCNT/PC bilayers with multiple light illumination ( $\text{mWcm}^{-2}$ ), fast response ( $\sim 0.5\text{ s}$ ), and wavelength-selective response. Hu et al. also proposed electrically, and optically responsive soft robots composed of tubular CNT/polymer bilayers [44]. In particular, they developed soft jumping robots actuated via light irradiation (Figure 2B). They reported that the light-driven energy accumulation in CNT parts was released instantaneously (3.56 s), leading to the mechanical shape deformation for the jumping motion. They utilized the photothermal ability in the CNT layer to absorb and convert it to thermal energy to heat up the polymer layer. These unique electrical and optical properties of CNTs can be utilized to develop a new class of

highly versatile applications, such as smart actuators, sensors, and oscillators. We discuss in detail potential applications of multi-functional materials combined with stimuli-responsive soft robots in the application section. Yamada et al. also introduced a new type of highly stretchable thin film composed of single-walled carbon nanotubes (SWCNTs) and poly(dimethylsiloxane) (PDMS) (Figure 2C) [45]. They reported that the SWCNT/PDMS thin films exhibited extraordinary durability and stability at high strain levels for ~3300 mechanical loading and unloading cycles. In particular, they proposed that their SWCNT/PDMS thin films could be utilized as wearable strain sensors that display high stretchability and sensitivity with fast response and low creep properties.

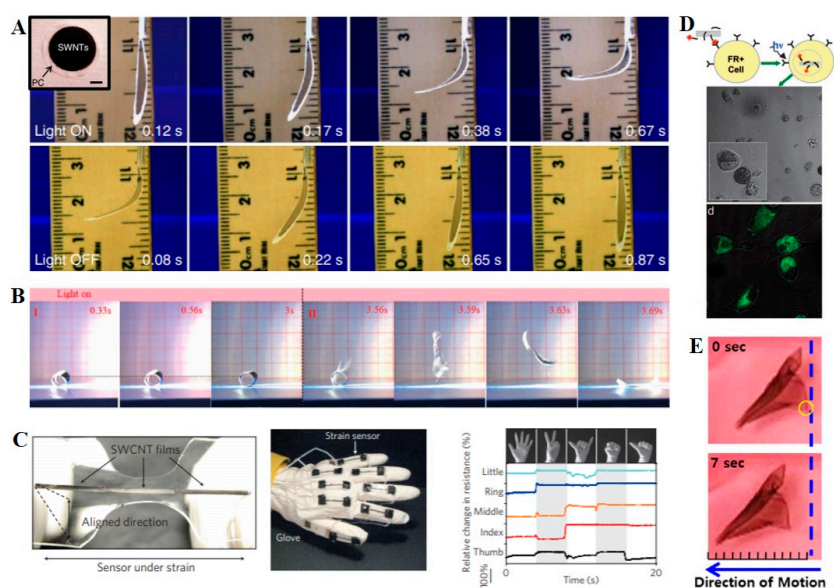


**Figure 2.** (A) Light responsive actuation of bilayers composed of polycarbonate (PC) and HiPCO nanotubes. Reproduced with permission [43], copyright 2014, Nature Publishing Group. (B) Light-responsive soft jumping robots composed of rolled carbon nanotube (CNT) and polymer bilayers. Reproduced with permission [44], copyright 2017, Wiley-VCH. (C) Carbon nanotube film-based strain sensor. Reproduced with permission [45], copyright 2011, Nature Publishing Group. (D) Single-walled carbon nanotube (SWCNT) transporter delivering DNA inside living cells. Reproduced with permission [46], copyright 2005, National Academy of Sciences. (E) Spontaneous motion of a triangular biohybrid swimmer composed of CNTs-gelatin methacrylate (GelMA). Reproduced with permission [47], copyright 2013, American Chemical Society.

Moreover, carbon nanotubes (CNTs) have shown multifunctionalities, which are capable of being utilized in biological systems [46,47]. For example, Kam et al. developed biological cargo systems using single-walled carbon nanotubes (SWCNTs) functionalized with phospholipid (PL)-polyethylene glycol (PEG) molecules [46]. They particularly demonstrated the selective targeting and killing of cancer cells by using functionalized SWCNTs via the PL-PEG-folic acid (FA) terminal group (Figure 2D). They developed SWCNT functionalization schemes with specific ligands recognizing and destroying tumor cells with low laser power ( $1.4 \text{ W/cm}^2$ ) and short radiation times, which is possible due to the high near-infrared (NIR) absorbance properties of carbon nanotubes. Moreover, Shin et al. fabricated CNT-embedded gelatin methacrylate (GelMA) cardiac patches [47]. They demonstrated that GelMA hydrogels significantly improve electrophysiological and mechanical properties with the addition of multi-walled CNTs. They systematically adjusted the mechanical modulus and electrical conductivity of the GelMA hydrogel based on their dependence on different CNT concentrations. They engineered CNT-GelMA triangular biohybrid actuators that can swell spontaneously under electrical stimulation (Figure 2E). They exhibited highly linear displacement of the CNT-GelMA swimmer under a square waveform of  $1 \text{ V/cm}$ , frequency of  $0.5\text{--}3 \text{ Hz}$ , and  $50 \text{ ms}$  pulse width. They proposed

advanced CNT-embedded GelMA cardiac constructs and bioactuators together by utilizing the fibrous morphologies and excellent optical, electrical, and mechanical properties of CNTs.

### 2.3. Graphene/Graphene Oxides (GO)-Stimuli-Responsive Composite Gels

Regarding the multi-functional and multi-environmental responsive shape-changing soft robots, stimuli-responsive materials have been combined with carbon-based materials, such as graphene, graphene oxide sheets (GOs), or their hybrids due to their high electrical, thermal, and optical properties [48–54]. To fold, bend, or roll two-dimensional atomic scale paper, various elegant scientific and engineering strategies have been developed. For example, Teshima et al. introduced a swift and easy way to spontaneously bend or roll thin poly (chloro-p-xylylene) (parylene-C) film by transferring monolayer graphene onto the parylene thin layer (Figure 3A) [48]. They demonstrated that the self-folding actuation of this bilayer was induced by reconfiguration of the molecules within the crystalline graphene, and other elements, such as 2D geometry design and thickness. They developed various spatial 3D geometries and transformed flower-shaped graphene/parylene-C bilayers into cage-shaped grippers that were expected to be utilized for the encapsulation and manipulation of living cells. Wang et al. proposed a photo-thermal responsive actuator using reduced graphene oxide (rGO) nanosheets and elastin-like polypeptides (ELPs) (Figure 3B) [49]. They fabricated a finger-shaped hydrogel machine, and its joint section was folded under an NIR laser spot similar to real hands. They developed bending direction manipulation by rastering the laser in a line across a hydrogel in different directions. Furthermore, the crawling functioned actuator was produced, and it moved forward by approximately 3 mm for each cycle.

Miskin et al. proposed origami fabrication using graphene sheets, silicon dioxide, and rigid panels of a photoresist (Figure 3C) [50]. Their graphene–glass biomorphs consisted of two parts: the folding and unfolded-flat. The rigid panels acted as a flat part during the attachment of graphene sheets and silicon oxide by non-reacting to stimuli, such as pH or heat. However, the folding parts consisting of graphene sheets and silicon oxide, not combined with rigid panels, can react to such stimuli. Moreover, they developed numerous 3D structures using these bimorphs at the micro scale, such as book shapes and mountain-valley shapes. Mu et al. proposed another fast self-folding origami using functionalized graphene oxide (GO) (Figure 3D) [51]. Specifically, they programmed dual vertical and lateral gradients to the GO nanoscale building blocks, which could shape-change in a few seconds. They observed that the nanostructures absorbed and desorbed water easily through photothermal triggering. In addition, they showed that the cross-shaped graphene paper could fold and unfold itself reversibly under near-infrared (NIR) light on/off processes with the rising and drop in temperature, respectively.

Xu et al. proposed a flexible self-folding platform using graphene and silver nanocubes (Ag NCs) in poly *N*-isopropylacrylamide (PNIPAM) hydrogels (Figure 3E) [52]. They developed a thermally responsive self-folding and encapsulating actuator. They demonstrated that the hybrid graphene skin wrapped MDA-MB-231-breast cancer cells, which adhered well to this graphene skin. The temperature (37 °C) of the cell culture was sufficient to induce the folding of the thermal-responsive skin. Joung et al. proposed another self-assembly process of 2D materials into 3D structures using graphene/graphene oxides (GOs) (Figure 3F) [53]. They selected a photo definable SU8 epoxy as a frame to support the graphene membranes with SPR 220 photoresist polymer hinges. They pointed out that the graphene/GOs structures self-fold when heated up to 100 °C to the melting point of SPR 220 hinges, which generates a surface tension force that induces a 3D self-assembly process. In particular, they demonstrated a self-folding cubic-shaped structure that possessed nontrivial spatial distribution of electron fields due to 3D plasmon hybridization.

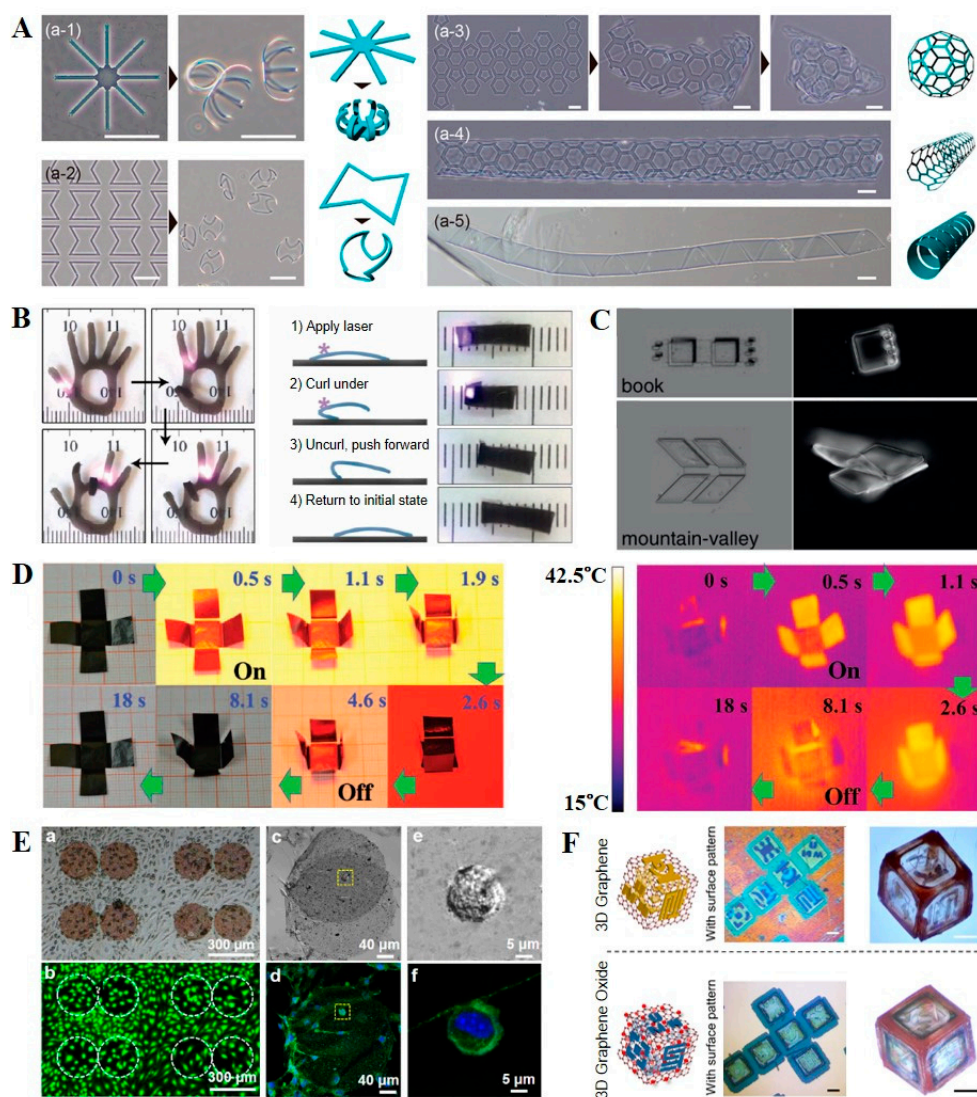


**Figure 3.** (A) Spontaneously bending or rolling thin poly (chloro-p-xylylene) (parylene-C) film through the transferring monolayer graphene process. Reproduced with permission [48], copyright 2018, American Chemical Society. (B) Controlled motion of hydrogel actuators composed of reduced graphene oxide (rGO) nanosheets. Reproduced with permission [49], copyright 2013, American Chemical Society. (C) Microscale graphene-glass bimorph three-dimensional (3D) structures. Reproduced with permission [50], adapted with permission under the terms of the Creative Commons Attribution Non Commercial License 4.0, copyright 2018, the authors. (D) A self-folding box driven by a light. Reproduced with permission [51], adapted with permission under the terms of the Creative Commons Attribution Non Commercial License 4.0, copyright 2015, the authors. (E) Wrapping of live breast cancer cells inside the G-PNIPAM-G-Ag skin. Reproduced with permission [52], copyright 2018, American Chemical Society. (F) 2D nets and 3D self-assembled graphene and graphene oxide (GO)-based cubes with surface patterns. Reproduced with permission [53], copyright 2017, American Chemical Society.

#### 2.4. MoS<sub>2</sub>-Stimuli-Responsive Composite Gels

Meanwhile, a semiconductor, molybdenum disulfide (MoS<sub>2</sub>), has demonstrated its relevant functionality to stimuli-responsive soft robots as intelligent actuators, sensors, and phototransistors. For specific examples, Lei et al. proposed a dual-responsive flexible actuator based on MoS<sub>2</sub> when exposed to heat and light sources (Figure 4A) [55]. They developed a thermally responsive actuator utilizing a tough poly *N*-isopropylacrylamide (PNIPAM) hydrogel matrix with a tunable volume phase transition temperature (VPTT). They fabricated a self-folding robot controlled by an untethered NIR

laser. In particular, they demonstrated that each anisotropic architecture part of the soft machine can bend when lights are applied and can finally grab a ball. In addition, they further observed that the MoS<sub>2</sub>-based hydrogel actuator could retain its shape even after the lights were turned off. The property regarding the generation of mechanical force is also an important factor for actuators if they have to catch something and retain its state. Acere et al. proposed electrode films made of 1T MoS<sub>2</sub> [56]. The films are capable of lifting masses that are more than 150 times that of the electrode over several millimeters and for hundreds of cycles when the voltage from  $-0.3$  V to  $+0.3$  V is applied. It can generate about 17 MPa of mechanical stresses and is also fully reversible and stable in a broad frequency range. The thin films are able to change the curving direction and degree of curvature by the intercalation of charging and discharging. Recently, Xu et al. also proposed reversibly actuated three-dimensional (3D) optoelectronic structures based on monolayer MoS<sub>2</sub> (Figure 4B) [57]. They designed differentially photo-crosslinked thin polymer (SU8) films for swelling gradients, which resulted in self-folding in the solvent exchange environment. In particular, they fabricated a photodetector composed of MoS<sub>2</sub>, Au electrodes, and SU8 films using various high-throughput fabrication methods, such as photolithography, thermal evaporation, and direct MoS<sub>2</sub> transfer. They demonstrated that the diverse MoS<sub>2</sub>/SU8 composite structures were self-folded when immersed in aqueous environments.

### 2.5. Liquid Crystals-Stimuli-Responsive Composite Gels

Liquid crystals mainly consist of liquid crystal elastomers (LCEs) or liquid crystal polymer networks (LCNs) that can transform into smart shapes when exposed to external stimuli, such as heat and light [58]. In general, the stimuli-responsive shape morphing of LCN- or LCE-based structures is based on the alignment of molecules (e.g., twisted nematic and splay configuration) and crosslinking density [59]. These stimuli-responsive liquid crystalline-based soft robots have been developed by specifically tuning the photo aligning properties. For example, Ware et al. designed mechanically multi-stable and shape-programmable soft actuators composed of LCE films (Figure 4C) [60]. They developed a remarkable strategy to imprint topological defects inside LCEs, which can display heterogeneous reversible shape morphing according to defect displacement and temperature. They particularly developed spontaneous and reversible actuating 3D soft robots composed of LCEs by controlling the surface alignment and crosslinking density. Additionally, Yu et al. developed a liquid crystalline embedded polymeric thin film that shows programmable directed bending through the orientation of linearly polarized light (Figure 4D) [61]. They showed that the bending direction of the LCN film moves anticlockwise by  $0^\circ$ ,  $45^\circ$ ,  $90^\circ$ , and  $135^\circ$  along with the polarization direction of light at 366 nm to  $0^\circ$ ,  $-45^\circ$ ,  $-90^\circ$ , and  $-135^\circ$ , respectively. Moreover, they demonstrated that the bending of LCN films reversibly turned back flat by using visible light with wavelengths longer than 540 nm. Recently, Liu et al. invented another smart, humid responsive soft actuator composed of cross-linked liquid crystal polymers (Figure 4E) [62]. They developed LCN films demonstrating a worm-line motion via humidity gradients. Specifically, they observed that the bottom surface could absorb more moisture than the top surface, which underwent asymmetric swelling along the thickness, in order for the LCN films to be bent or rolled.

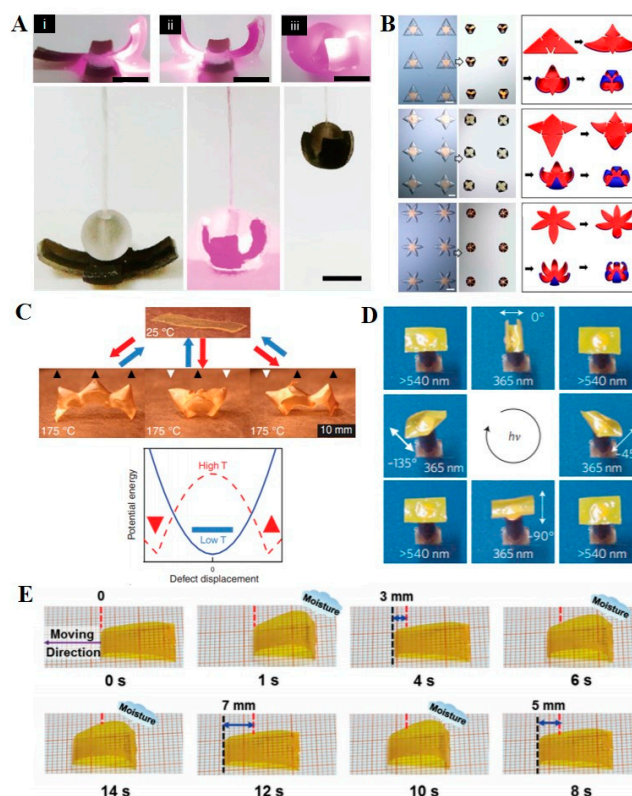


**Figure 4.** (A) Flexible anisotropic actuator upon near-infrared (NIR) irradiation from the flat to folded shapes. Reproduced with permission [55], copyright 2016, Royal Society of Chemistry. (B) Self-folding molybdenum disulfide ( $\text{MoS}_2$ )–SU8 structures with different shapes. Reproduced with permission [57], copyright 2019, American Chemical Society. (C) Thermally responsive liquid crystal elastomer (LCE) with mechanical multi-stability. Reproduced with permission [60], copyright 2015, AAAS. (D) Photoinduced soft actuators composed of liquid crystal polymer networks (LCNs). Reproduced with permission [61], copyright 2015, Nature Publishing Group. (E) Humidity-induced actuator composed of crosslinked liquid crystal polymers (CLCPs). Reproduced with permission [62], copyright 2017, Wiley-VCH.

### 3. Applications of Hybrid Soft Robots

A variety of futuristic applications of stimuli-responsive soft robots have been proposed in the forms of flexible electronics, sensors, biomedical tools, optics, and actuators [1–7,24–26]. Furthermore, hybrid stimuli-responsive soft robots combined with multi-functional nanoparticles, low-dimensional materials, or liquid crystals have also displayed promising applications in flexible electronics, mechanical sensors, smart actuators, and biomedical systems [18–21,23–28]. This section particularly describes advanced applications of hybrid stimuli-responsive soft robots focusing on extensively multi-responsive and multi-functional actuators (e.g., manipulators, grippers, and walkers) and sensors (e.g., wearable electronics, strain sensors, biosensors, and gas sensors).

#### 3.1. Hybrid Soft Actuators

Hybrid stimuli-responsive soft robots have been extensively validated as multi-functional and multi-responsive smart soft actuators or manipulators. While many soft actuators have been developed, most of them can only respond to mono-stimulus, and it is difficult to develop multi-responsive and functional advanced soft actuators. To overcome these limitations, many functional materials such as carbon-based materials, nanowires, and liquid crystals have been hybridized with stimuli-responsive soft actuators. For example, Xu et al. proposed a self-folding 3D graphene actuator combined with a thermally responsive poly *N*-isopropylacrylamide (PNIPAM) hydrogel [63]. They particularly

developed an elegant strategy to fold and unfold the ultrathin atomic scale graphene layer reversibly by utilizing self-foldable PNIPAM-based precursors induced by the temperature increase and decrease processes. Regarding the formation of a smart soft actuating system, they fabricated a thermally responsive hybrid flower-shaped gripper that could encapsulate live cells specifically through the heating/cooling processes, which has proven the concept of futuristic application of smart untethered microscale gripping robots in biomedical engineering (Figure 5A). Ma et al. introduced a thermally responsive biomimetic flower-shaped actuator with color-tunable fluorescence functions (Figure 5B) [64]. As described previously, to generate mechanical deformation, such as bending, rolling, wrinkling, or folding, many geometrical strategies that generate gradients have to be developed. Among many strategies to obtain shape transformation, bilayer systems composed of heterogeneous properties are primarily considered to exhibit time-dependent shape transformation when exposed to external environments. More comprehensive reviews for diverse mechanisms of shape transformation have been introduced [2,6,16,21]. In particular, they developed an anisotropic bilayer actuator composed of graphene oxide (GO)/poly(*N*-isopropylacrylamide) (PNIPAM) and perylene bisimide-functionalized hyperbranched polyethylenimine (PBI-HPEI). They specifically accomplished dual thermal and pH-responsive smart bilayer soft actuators with color-changing functions.

The heat source is one of the easily adapted conventional triggering sources to generate the shape transformation of soft actuators. Due to the high electric-to-thermal transferring properties of nanowires and nanoparticles, most shape-changing hybrid soft actuators are capable of being operated via heating up and cooling down processes. However, the heat source has a limitation of having to be utilized selectively at the specified areas due to its continuous reactivity. To overcome this limitation, another feasible approach to increase the selectivity of a stimulus at the local positions is to manage the optical properties of stimuli sources. The light is untethered and can be controlled from an exterior side of the systems. Along with this optical advantage, photo-to-thermal responsive multi-functional soft robots have been extensively developed [41,65–73]. For example, Cheng et al. developed a rectangular-shaped graphene oxide (GO) film walker in response to an infrared (IR) light on/off process (Figure 5C) [65]. They demonstrated that the walker could move on a ratchet paper via an IR light-induced thermal response from the GO film. Furthermore, they exhibited a simple way to fabricate a GO-based walker by direct casting along with verifying the multi reactivity of the walker via external heat, light, and moisture cues. These optically responsive LCEs and LCNs have also been extensively combined with stimuli-responsive materials to form multi-functional advanced soft robots [66,73–77]. Wani et al. demonstrated a light-driven actuator composed of LCEs, for example (Figure 5D) [66]. It is essential to know that the shape transformation of the LCE-based actuator is based on tuning the alignment of molecules within the LCEs when exposed to the light source [78,79]. Using a similar approach, they fabricated a light-induced splay-aligned LCE actuator with a transparent optical fiber attachment at the center position for the path of emitted light.

In addition, a chemically responsive actuator can be operated by the transformation of chemical energy into mechanical energy as a chemomechanical deformation [24,74]. Stimuli-responsive polymers, hydrogels, or hybrids of them have the ability to locally and selectively diffuse targeted chemicals in-and-out and reversibly. This diffusion can be induced by external cues, such as organic solvents, ionic strengths, acids, bases, and water molecules. These external triggers involve a variety of chemical reactions inside a material system that causes mechanical stress, allowing the shape transformation of soft robots. Recently, chemically responsive soft actuators have also been developed by integrating multi-functional materials. Deng et al. introduced solvent-driven self-folding graphene/SU8 bilayer structures (Figure 5E) [80]. They developed a new method to combine multi-functional graphene-based materials with a stimuli-responsive SU8 photoresist. Specifically, they patterned crosslinking gradients SU8 onto few-layered graphene (FLG), which displayed self-bending, -folding, or -rolling when immersed in acetone. In addition, the FLG/SU8 bilayer structures could reversibly flatten when exposed to water. This self-folding mechanism of FLG/SU8 is rationalized by the fact that low UV light

exposure generates crosslink gradients along a thickness, and thus less-crosslinked areas display large mass changes compared to the completely crosslinked areas during acetone conditioning [81].

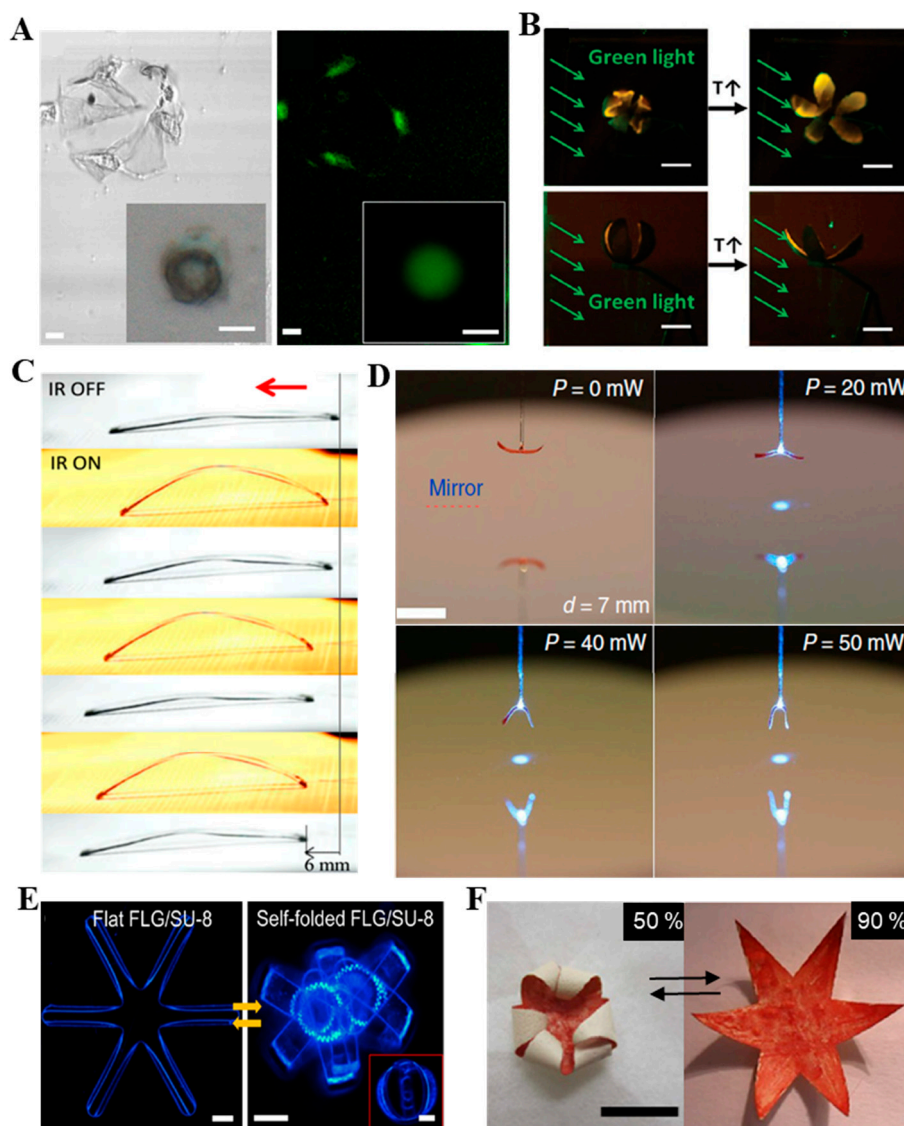


**Figure 5.** (A) Encapsulation of live cells within the functionalized flower-shaped thermally responsive graphene/poly *N*-isopropylacrylamide (PNIPAM) gripper. Reproduced with permission [63], adapted with permission under the terms of the Creative Commons Attribution Non Commercial License 4.0, copyright 2017, the authors. (B) Thermally responsive flower-shaped color displaying soft actuator. Reproduced with permission [64], copyright 2018, Wiley-VCH. (C) GO film walker in response to the IR on/off processes. Reproduced with permission [65], copyright 2016, American Chemical Society. (D) A light driven liquid crystalline elastomer (LCE)-based biomimetic flytrap gripper. Reproduced with permission [66], adapted with permission under the terms of the Creative Commons Attribution Non Commercial License 4.0, copyright 2017, the authors. (E) Solvent-driven soft gripper composed of few-layered graphene (FLG)/SU8 bilayers. Reproduced with permission [80], copyright 2015, AIP publishing. (F) Multi-responsive ionic polymer actuator driven by solvent molecule absorption/desorption processes. Reproduced with permission [82], copyright 2014, Nature Publishing Group.

Hybrid stimuli-responsive actuators can also react to water. Humidity driven hydrogel actuators have been reported as biomimetic walkers, grippers, or artificial muscles [6,20,36,83–87]. Similar to the opening and closing systems of plants [88–90], biomimetic hybrid stimuli-responsive soft robots can

bend, fold, or curl due to changes in humidity. For example, Zhao et al. introduced a multi-responsive polymer actuator that exhibited reversible closing and opening of a biomimetic flower-shaped actuator in response to humidity (Figure 5F) [82]. They also demonstrated that the membrane was rolled and flattened in acetone vapor and air exposure, respectively.

### 3.2. Stimuli-Responsive Hybrid Sensors

Hybrid stimuli-responsive soft robots have also extensively addressed the key possible applications of smart mechanical stress/strain sensors [31,40,91–97]. First, hybrid stimuli-responsive soft robots are advantageous for smart sensors because of their extensive shape-changing capabilities. For example, Amjadi et al. proposed a cost-effective stretchable strain sensor based on a reversible microcrack in graphite thin films (Figure 6A) [98]. They demonstrated that the high performance of sensors was developed by self-organized microcracks in films coated on soft elastomer films and acrylic plates. They further reported that their strain sensors detected deformation from 0.1% to more than 50% with high sensitivity and different distinguished sound intensities. Thus, they suggested that this strain sensor could be utilized for relatively stronger stress points, such as the joint movement of a finger. They finally proposed that it could be employed for monitoring human physiological activity with significantly low hysteresis. In addition, Choi et al. proposed another ionic-liquid-based strain sensor (Figure 6B) [99]. They combined ethylene glycol and sodium chloride as the ionic liquids. They particularly developed an ionic-liquid-based wavy (ILBW) sensor that showed a low value of hysteresis (0.15% at 250%) compared to other strain sensors based on the same materials. They utilized a wavy fluidic channel to diminish the hysteresis of the sensor. Moreover, they demonstrated that the ILBW sensor showed a high performance of low overshoot (1.7% at 150% strain) and high reversibility (3000 cycles at 300% strain). In addition to graphene oxide-based or ionic liquid-based sensors, Li et al. described a highly stretchable and conductive hybrid strain sensor composed of thermoplastic polyurethane (TPU), multi-walled carbon nanotubes (MWNTs), and single-walled carbon nanotubes (SWCNTs) (Figure 6C) [100]. They observed that when it was fully stretched, the relative resistance increased and reached a maximum value, and it decreased at its relaxation state. They noticed that the TPU/MWNT/SWCN composite sensor specifically possessed high stretchability, a large workable strain range (100%), and great cycle stability (2000 cycles). Finally, they applied this highly conductive and stretchable sensor for monitoring human joint motion as wearable strain sensors or wearable textile electronics without any assistance.

In addition, the excellent chemical and optoelectrical properties of functional materials have exhibited potential for advanced possibilities when combined with the stimuli-responsive soft robots. For example, Xing et al. developed a chemically responsive nano-junction using electro-migration of a silver nanowire (Figure 6D) [101]. They demonstrated that exposing the chemically responsive junction (CRJ) nanowire to ammonia ( $\text{NH}_3$ ), water vapor, or nitrogen dioxide ( $\text{NO}_2$ ) induced reversible resistance change from  $-10\%$  to  $138\%$ . They fabricated a nanogap between the CRJ nanowire via electro-migration with a minimum width of 5 nm. In particular, the chemical sensor was expected to increase the selectivity for the detection of specific molecules of highly miniaturized sensors or sensor arrays. In addition, Lopez-Sanchez et al. proposed ultrasensitive photodetectors using single layers of  $\text{MoS}_2$  and other silicon or silicon oxide substrates. (Figure 6E) [102].

Due to the direct bandgap of the  $\text{MoS}_2$  monolayer, a photo-responsivity of  $880 \text{ AW}^{-1}$  can be achieved, which is a significant improvement over former  $\text{MoS}_2$  monolayer phototransistors. The device responded to voltage induced by two gold electrodes (90 nm thick) only when the laser light ( $\lambda = 561 \text{ nm}$ ) was turned on with an illumination power of  $15 \mu\text{W}$ . When four different bias voltages (from 1 V to 8 V) were applied, there was a difference in the trend of the photocurrent's increase and decrease after the laser beam was switched on/off. The device exhibited the potential to be utilized in sensors for fluorescence imaging and fabrication of inexpensive, highly sensitive, and flexible  $\text{MoS}_2$  optoelectronic devices. This chemical or optoelectrical sensitivity of multi-functional

nanowires, nanoparticles, and two-dimensional materials has demonstrated the possibility for the development of more advanced stimuli-responsive hybrid chemical and optoelectrical sensors.

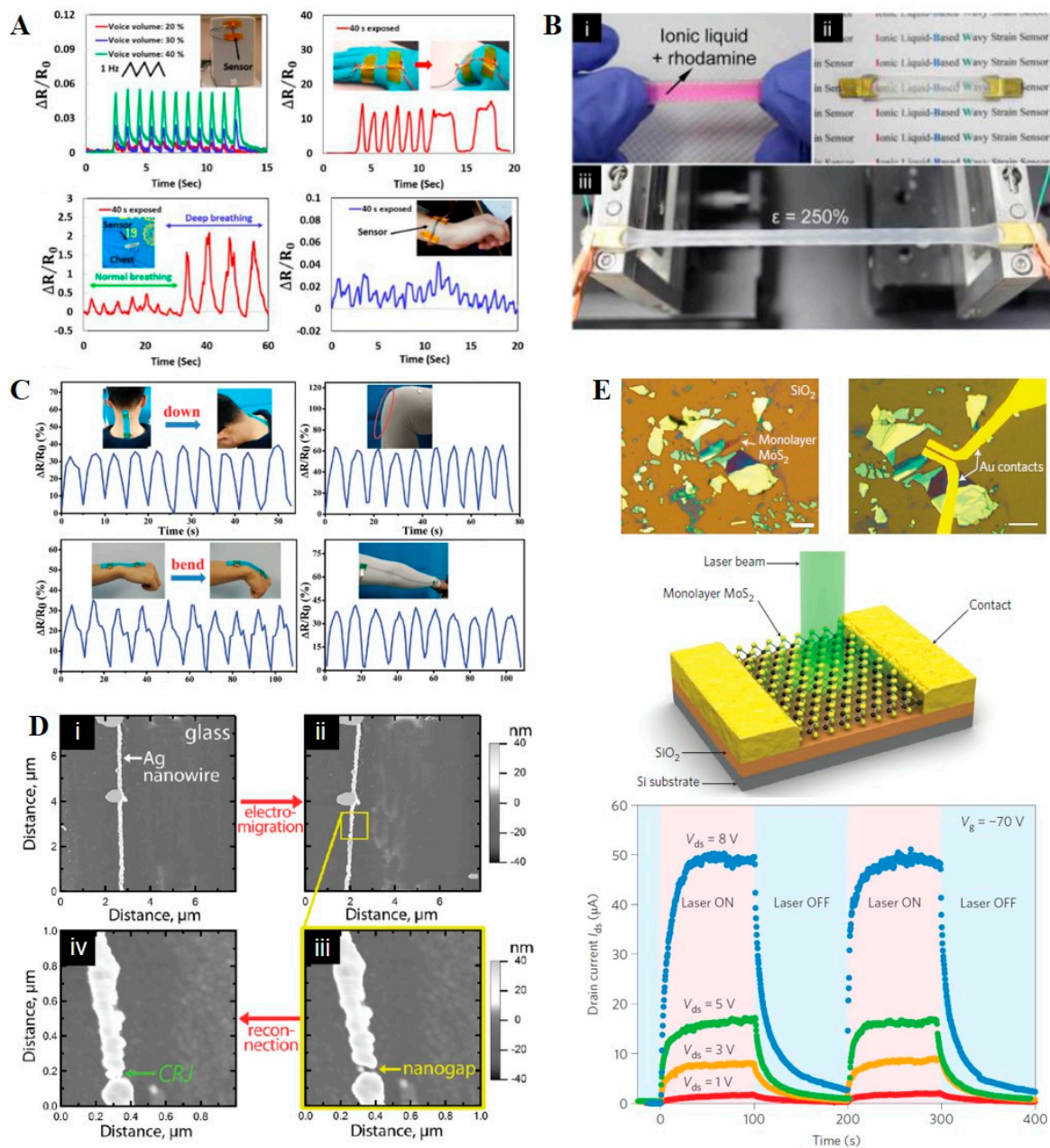


**Figure 6.** (A) Low-strain and large-strain application demonstrations of the proposed strain sensors. Reproduced with permission [98], copyright 2016, American Chemical Society. (B) Ionic-liquid-based wavy (ILBW) strain sensor, indicating its (i) wavy structure, (ii) good transparency, and (iii) super-stretchability. Reproduced with permission [99], copyright 2017, American Chemical Society. (C) Monitoring of human motion using the SWNT/multi-walled carbon nanotube (MWNT)/thermoplastic polyurethane (TPU) yarn (SMTY) strain sensors. Reproduced with permission [100], copyright 2018, Royal Society of Chemistry. (D) Tracking the formation of a chemically responsive junction (CRJ) using AFM. Reproduced with permission [101], copyright 2012, American Chemical Society. (E) Monolayer MoS<sub>2</sub> phototransistor layout and photocurrent dynamics. Reproduced with permission [102], copyright 2013, Nature Publishing Group.

In addition, MoS<sub>2</sub> is the proper material for fabricating a sensor, especially a gas detector. Kim et al. presented a volatile organic compound (VOC) sensor by using thiolated ligand in conjugation with MoS<sub>2</sub> [103]. It is notable for the application of lung cancer diagnosis through breath analysis and because it highly sensitively showed positive responses to oxygen-functionalized VOCs. The normalized ranges of resistance changes can be characterized depending on the types of VOCs, such as toluene, hexane, ethanol, propionaldehyde, and acetone. Likewise, Kumar et al. proposed a sensor for detecting NO<sub>2</sub> gases [104]. They fabricated it based on MoS<sub>2</sub> grown by the chemical vapor deposition (CVD) technique and used photo-thermal energy with photo-excitation to enhance the sensitivity and response time compared to the state of room temperature with no lights. The sensor showed a relative response to 100 ppm of the gases with resistance change up to 30%, and it can react to the gas in about 29 s and recover completely at RT, under UV illumination.

Furthermore, MoS<sub>2</sub> has a lot of potential for useful E-skin, a wearable application. Park et al. demonstrated a prototype of the conformal MoS<sub>2</sub> tactile sensor [105]. They solved the problem regarding high hysteresis, nonlinearity, and poor repeatability in existing sensors through integrating MoS<sub>2</sub> with a graphene electrode. This ultrathin sensor shows mechanical flexibility over a strain of 1.98% and optical transparency over 80%. It can retain linearity in the relative resistance changes when the strain from −2% (compressive) to 2% (tensile) was applied and it can retain its reversibility after 10,000 cycles.

#### 4. Conclusions

Stimuli-responsive soft robots integrated with hybrid functional materials have attracted significant attention as a new class of intelligent systems applicable in multi-functional and multi-responsive actuators or sensors. Hybrid stimuli-responsive soft robots composed of nanomaterials, 2DLMs, or liquid crystals display excellent mechanical, electrical, chemical, and optical properties with programmable smart shape transformation when exposed to external environmental cues. However, there are many challenges impeding the practical applications of these robots. One of the challenges is that nonlinear abnormal effects, such as the snapping or bucking of stimuli-responsive soft robots, have not been extensively studied. Thus, the mechanical and chemical prediction of shape transformation must be studied together. In addition, the sensitivity feedback and response time from external cues have to be developed to obtain instantly reactive actuators, walkers, or sensors.

Most advanced hybrid stimuli-responsive soft robots stay within their conceptual states. To achieve integrated practically applicable soft robots, more precise navigation and transformation of these stimuli-responsive soft robots must be developed. In particular, multiscale stimuli-responsive soft robots have to be validated under further real environmental conditions, such as deep in vivo locations. To realize the autonomous navigation and transformation of hybrid stimuli-responsive soft robots, other rarely explored cues, such as ultrasound and magnetic resonance have to be studied as well in real models. To realize advanced multi-functional and multi-responsive hybrid soft robots, all material selections and synthesis, 3D fabrication strategies, and precise controlling systems have to be developed in parallel. Thus, hybrid stimuli-responsive soft robots offer significant prospects to facilitate the realization of intelligent multi-functional and multi-responsive soft actuators and sensors as smart soft robots.

**Author Contributions:** H.S. and C.Y. reviewed, analyzed, and wrote the paper. All authors have read and agreed to the published version of the manuscript.

**Funding:** This research was supported by Sookmyung Women's University Research Grant (1-1903-1104).

**Conflicts of Interest:** The authors declare no conflict of interest.

## References

1. Liu, X.; Liu, J.; Lin, S.; Zhao, X. Hydrogel machines. *Mater. Today* **2020**, *36*, 102–124. [[CrossRef](#)]
2. Erol, O.; Pantula, A.; Liu, W.; Gracias, D.H. Transformer Hydrogels: A Review. *Adv. Mater. Technol.* **2019**, *4*, 1900043. [[CrossRef](#)]
3. Ghosh, A.; Yoon, C.; Ongaro, F.; Scheggi, S.; Selaru, F.M.; Misra, S.; Gracias, D.H. Stimuli-Responsive Soft Untethered Grippers for Drug Delivery and Robotic Surgery. *Front. Mech. Eng.* **2017**, *3*, 7. [[CrossRef](#)] [[PubMed](#)]
4. Jeon, S.J.; Hauser, A.W.; Hayward, R.C. Shape-Morphing Materials from Stimuli-Responsive Hydrogel Hybrids. *Acc. Chem. Res.* **2017**, *50*, 161–169. [[CrossRef](#)]
5. Peraza-Hernandez, E.A.; Hartl, D.J.; Malak, R.J.; Lagoudas, D.C. Origami-inspired active structures: A synthesis and review. *Smart Mater. Struct.* **2014**, *23*, 094001. [[CrossRef](#)]
6. Ionov, L. Hydrogel-based actuators: Possibilities and limitations. *Mater. Today* **2014**, *17*, 494–503. [[CrossRef](#)]
7. Pilz da Cunha, M.; Debije, M.G.; Schenning, A.P.H.J. Bioinspired light-driven soft robots based on liquid crystal polymers. *Chem. Soc. Rev.* **2020**, *49*, 6568–6578. [[CrossRef](#)]
8. Zhang, Y.S.; Khademhosseini, A. Advances in engineering hydrogels. *Science* **2017**, *356*, eaaf3627. [[CrossRef](#)]
9. Ahn, S.; Kasi, R.M.; Kim, S.-C.; Sharma, N.; Zhou, Y. Stimuli-responsive polymer gels. *Soft Matter* **2008**, *4*, 1151–1157. [[CrossRef](#)]
10. Breger, J.C.; Yoon, C.; Xiao, R.; Kwag, H.R.; Wang, M.O.; Fisher, J.P.; Nguyen, T.D.; Gracias, D.H. Self-folding thermo-magnetically responsive soft microgrippers. *ACS Appl. Mater. Interfaces* **2015**, *7*, 3398–3405. [[CrossRef](#)]
11. Malachowski, K.; Breger, J.; Kwag, H.R.; Wang, M.O.; Fisher, J.P.; Selaru, F.M.; Gracias, D.H. Stimuli-responsive theragrippers for chemomechanical controlled release. *Angew. Chem. Int. Ed.* **2014**, *53*, 8045–8049. [[CrossRef](#)]
12. Fusco, S.; Sakar, M.S.; Kennedy, S.; Peters, C.; Bottani, R.; Starsich, F.; Mao, A.; Sotiriou, G.A.; Pané, S.; Pratsinis, S.E.; et al. An integrated microrobotic platform for on-demand, targeted therapeutic interventions. *Adv. Mater.* **2014**, *26*, 952–957. [[CrossRef](#)] [[PubMed](#)]
13. Hu, Z.; Zhang, X.; Li, Y. Synthesis and application of modulated polymer gels. *Science* **1995**, *269*, 525–527. [[CrossRef](#)] [[PubMed](#)]
14. Kim, J.; Yoon, J.; Hayward, R.C. Dynamic display of biomolecular patterns through an elastic creasing instability of stimuli-responsive hydrogels. *Nat. Mater.* **2010**, *9*, 159–164. [[CrossRef](#)]
15. Klein, Y.; Efrati, E.; Sharon, E. Shaping of elastic sheets by prescription of non-Euclidean metrics. *Science* **2007**, *315*, 1116–1120. [[CrossRef](#)] [[PubMed](#)]
16. Gracias, D.H. Stimuli responsive self-folding using thin polymer films. *Curr. Opin. Chem. Eng.* **2013**, *2*, 112–119. [[CrossRef](#)]
17. Stuart, M.A.C.; Huck, W.T.S.; Genzer, J.; Müller, M.; Ober, C.; Stamm, M.; Sukhorukov, G.B.; Szleifer, I.; Tsukruk, V.V.; Urban, M.; et al. Emerging applications of stimuli-responsive polymer materials. *Nat. Mater.* **2010**, *9*, 101–113. [[CrossRef](#)]
18. Kirillova, A.; Ionov, L. Shape-changing polymers for biomedical applications. *J. Mater. Chem. B* **2019**, *7*, 1597–1624. [[CrossRef](#)] [[PubMed](#)]
19. Yoon, C.K. Advances in biomimetic stimuli responsive soft grippers. *Nano Converg.* **2019**, *6*, 1–14. [[CrossRef](#)]
20. Ionov, L. Biomimetic hydrogel-based actuating systems. *Adv. Funct. Mater.* **2013**, *23*, 4555–4570. [[CrossRef](#)]
21. Le, X.; Lu, W.; Zhang, J.; Chen, T. Recent Progress in Biomimetic Anisotropic Hydrogel Actuators. *Adv. Sci.* **2019**, *6*, 1801584. [[CrossRef](#)] [[PubMed](#)]
22. Peng, X.; Wang, H. Shape changing hydrogels and their applications as soft actuators. *J. Polym. Sci. Part B Polym. Phys.* **2018**, *56*, 1314–1324. [[CrossRef](#)]
23. Ding, M.; Jing, L.; Yang, H.; Machnicki, C.E.; Fu, X.; Li, K.; Wong, I.Y.; Chen, P.Y. Multifunctional soft machines based on stimuli-responsive hydrogels: From freestanding hydrogels to smart integrated systems. *Mater. Today Adv.* **2020**, *8*, 100088. [[CrossRef](#)]
24. Hines, L.; Petersen, K.; Lum, G.Z.; Sitti, M. Soft Actuators for Small-Scale Robotics. *Adv. Mater.* **2017**, *29*, 1603483. [[CrossRef](#)] [[PubMed](#)]
25. Lee, Y.; Song, W.J.; Sun, J.Y. Hydrogel soft robotics. *Mater. Today Phys.* **2020**, *15*, 100258. [[CrossRef](#)]
26. Shen, Z.; Chen, F.; Zhu, X.; Yong, K.T.; Gu, G. Stimuli-responsive functional materials for soft robotics. *J. Mater. Chem. B* **2020**, *8*, 8972–8991. [[CrossRef](#)]

27. Kim, H.; Ahn, S.K.; Mackie, D.M.; Kwon, J.; Kim, S.H.; Choi, C.; Moon, Y.H.; Lee, H.B.; Ko, S.H. Shape morphing smart 3D actuator materials for micro soft robot. *Mater. Today* **2020**. [[CrossRef](#)]
28. Xu, W.; Gracias, D.H. Soft Three-Dimensional Robots with Hard Two-Dimensional Materials. *ACS Nano* **2019**, *13*, 4883–4892. [[CrossRef](#)]
29. Lee, J.; Oh, S.; Pyo, J.; Kim, J.M.; Je, J.H. A light-driven supramolecular nanowire actuator. *Nanoscale* **2015**, *7*, 6457–6461. [[CrossRef](#)]
30. Wu, J.; Zang, J.; Rathmell, A.R.; Zhao, X.; Wiley, B.J. Reversible sliding in networks of nanowires. *Nano Lett.* **2013**, *13*, 2381–2386. [[CrossRef](#)]
31. Liu, X.; Gao, H.; Ward, J.E.; Liu, X.; Yin, B.; Fu, T.; Chen, J.; Lovley, D.R.; Yao, J. Power generation from ambient humidity using protein nanowires. *Nature* **2020**, *578*, 550–554. [[CrossRef](#)] [[PubMed](#)]
32. Kim, H.; Lee, H.; Ha, I.; Jung, J.; Won, P.; Cho, H.; Yeo, J.; Hong, S.; Han, S.; Kwon, J.; et al. Biomimetic Color Changing Anisotropic Soft Actuators with Integrated Metal Nanowire Percolation Network Transparent Heaters for Soft Robotics. *Adv. Funct. Mater.* **2018**, *28*, 1801847. [[CrossRef](#)]
33. Li, K.; Shao, Y.; Yan, H.; Lu, Z.; Griffith, K.J.; Yan, J.; Wang, G.; Fan, H.; Lu, J.; Huang, W.; et al. Lattice-contraction triggered synchronous electrochromic actuator. *Nat. Commun.* **2018**, *9*, 1–11. [[CrossRef](#)] [[PubMed](#)]
34. Chen, P.; Shi, R.; Shen, N.; Zhang, Z.; Liang, Y.; Li, T.; Wang, J.; Kong, D.; Gan, Y.; Amini, A.; et al. Multistimuli-Responsive Insect-Scale Soft Robotics Based on Anisotropic Super-Aligned VO<sub>2</sub> Nanowire/Carbon Nanotube Bimorph Actuators. *Adv. Intell. Syst.* **2020**, *2000051*, 2000051. [[CrossRef](#)]
35. Kim, H.; Lee, J.A.; Sim, H.J.; Lima, M.D.; Baughman, R.H.; Kim, S.J. Temperature-Responsive Tensile Actuator Based on Multi-walled Carbon Nanotube Yarn. *Nano Micro Lett.* **2016**, *8*, 254–259. [[CrossRef](#)]
36. Gu, X.; Fan, Q.; Yang, F.; Cai, L.; Zhang, N.; Zhou, W.; Zhou, W.; Xie, S. Hydro-actuation of hybrid carbon nanotube yarn muscles. *Nanoscale* **2016**, *8*, 17881–17886. [[CrossRef](#)]
37. Mahapatra, S.S.; Yadav, S.K.; Yoo, H.J.; Ramasamy, M.S.; Cho, J.W. Tailored and strong electro-responsive shape memory actuation in carbon nanotube-reinforced hyperbranched polyurethane composites. *Sens. Actuators B Chem.* **2014**, *193*, 384–390. [[CrossRef](#)]
38. Hu, Y.; Chen, W.; Lu, L.; Liu, J.; Chang, C. Electromechanical actuation with controllable motion based on a single-walled carbon nanotube and natural biopolymer composite. *ACS Nano* **2010**, *4*, 3498–3502. [[CrossRef](#)]
39. Zhang, X.; Pint, C.L.; Lee, M.H.; Schubert, B.E.; Jamshidi, A.; Takei, K.; Ko, H.; Gillies, A.; Bardhan, R.; Urban, J.J.; et al. Optically- and thermally-responsive programmable materials based on carbon nanotube-hydrogel polymer composites. *Nano Lett.* **2011**, *11*, 3239–3244. [[CrossRef](#)]
40. Lee, J.; Pyo, S.; Kwon, D.S.; Jo, E.; Kim, W.; Kim, J. Ultrasensitive Strain Sensor Based on Separation of Overlapped Carbon Nanotubes. *Small* **2019**, *15*, 1805120. [[CrossRef](#)]
41. Li, H.; Wang, J. Ultrafast yet Controllable Dual-Responsive All-Carbon Actuators for Implementing Unusual Mechanical Movements. *ACS Appl. Mater. Interfaces* **2019**, *11*, 10218–10225. [[CrossRef](#)] [[PubMed](#)]
42. Yamamoto, Y.; Kanao, K.; Arie, T.; Akita, S.; Takei, K. Air Ambient-Operated pNIPAM-Based Flexible Actuators Stimulated by Human Body Temperature and Sunlight. *ACS Appl. Mater. Interfaces* **2015**, *7*, 11002–11006. [[CrossRef](#)] [[PubMed](#)]
43. Zhang, X.; Yu, Z.; Wang, C.; Zarrouk, D.; Seo, J.W.T.; Cheng, J.C.; Buchan, A.D.; Takei, K.; Zhao, Y.; Ager, J.W.; et al. Photoactuators and motors based on carbon nanotubes with selective chirality distributions. *Nat. Commun.* **2014**, *5*, 1–8. [[CrossRef](#)] [[PubMed](#)]
44. Hu, Y.; Liu, J.; Chang, L.; Yang, L.; Xu, A.; Qi, K.; Lu, P.; Wu, G.; Chen, W.; Wu, Y. Electrically and Sunlight-Driven Actuator with Versatile Biomimetic Motions Based on Rolled Carbon Nanotube Bilayer Composite. *Adv. Funct. Mater.* **2017**, *27*, 1704388. [[CrossRef](#)]
45. Yamada, T.; Hayamizu, Y.; Yamamoto, Y.; Yomogida, Y.; Izadi-Najafabadi, A.; Futaba, D.N.; Hata, K. A stretchable carbon nanotube strain sensor for human-motion detection. *Nat. Nanotechnol.* **2011**, *6*, 296–301. [[CrossRef](#)] [[PubMed](#)]
46. Kam, N.W.S.; O'Connell, M.; Wisdom, J.A.; Dai, H. Carbon nanotubes as multifunctional biological transporters and near-infrared agents for selective cancer cell destruction. *Proc. Natl. Acad. Sci. USA* **2005**, *102*, 11600–11605. [[CrossRef](#)] [[PubMed](#)]
47. Shin, S.R.; Jung, S.M.; Zalabany, M.; Kim, K.; Zorlutuna, P.; Kim, S.B.; Nikkhah, M.; Khabiry, M.; Azize, M.; Kong, J.; et al. Carbon-nanotube-embedded hydrogel sheets for engineering cardiac constructs and bioactuators. *ACS Nano* **2013**, *7*, 2369–2380. [[CrossRef](#)]

48. Teshima, T.F.; Henderson, C.S.; Takamura, M.; Ogawa, Y.; Wang, S.; Kashimura, Y.; Sasaki, S.; Goto, T.; Nakashima, H.; Ueno, Y. Self-Folded Three-Dimensional Graphene with a Tunable Shape and Conductivity. *Nano Lett.* **2019**, *19*, 461–470. [[CrossRef](#)]
49. Wang, E.; Desai, M.S.; Lee, S.W. Light-controlled graphene-elastin composite hydrogel actuators. *Nano Lett.* **2013**, *13*, 2826–2830. [[CrossRef](#)]
50. Miskin, M.Z.; Dorsey, K.J.; Bircan, B.; Han, Y.; Muller, D.A.; McEuen, P.L.; Cohen, I. Graphene-based bimorphs for micron-sized, tautonomous origami machines. *Proc. Natl. Acad. Sci. USA* **2018**, *115*, 466–470. [[CrossRef](#)]
51. Mu, J.; Hou, C.; Wang, H.; Li, Y.; Zhang, Q.; Zhu, M. Origami-inspired active Graphene-Based paper for programmable instant self-folding walking devices. *Sci. Adv.* **2015**, *1*, e1500533. [[CrossRef](#)] [[PubMed](#)]
52. Xu, W.; Paidi, S.K.; Qin, Z.; Huang, Q.; Yu, C.-H.; Pagaduan, J.V.; Buehler, M.J.; Barman, I.; Gracias, D.H. Self-Folding Hybrid Graphene Skin for 3D Biosensing. *Nano Lett.* **2018**, *19*, 1409–1417. [[CrossRef](#)] [[PubMed](#)]
53. Joung, D.; Nemilentsau, A.; Agarwal, K.; Dai, C.; Liu, C.; Su, Q.; Li, J.; Low, T.; Koester, S.J.; Cho, J.H. Self-Assembled Three-Dimensional Graphene-Based Polyhedrons Inducing Volumetric Light Confinement. *Nano Lett.* **2017**, *17*, 1987–1994. [[CrossRef](#)] [[PubMed](#)]
54. Tang, Z.; Gao, Z.; Jia, S.; Wang, F.; Wang, Y. Graphene-Based Polymer Bilayers with Superior Light-Driven Properties for Remote Construction of 3D Structures. *Adv. Sci.* **2017**, *4*, 1600437. [[CrossRef](#)] [[PubMed](#)]
55. Lei, Z.; Zhu, W.; Sun, S.; Wu, P. MoS<sub>2</sub>-based dual-responsive flexible anisotropic actuators. *Nanoscale* **2016**, *8*, 18800–18807. [[CrossRef](#)] [[PubMed](#)]
56. Acerce, M.; Akdoan, E.K.; Chhowalla, M. Metallic molybdenum disulfide nanosheet-based electrochemical actuators. *Nature* **2017**, *549*, 370–373. [[CrossRef](#)]
57. Xu, W.; Li, T.; Qin, Z.; Huang, Q.; Gao, H.; Kang, K.; Park, J.; Buehler, M.J.; Khurgin, J.B.; Gracias, D.H. Reversible MoS<sub>2</sub> Origami with Spatially Resolved and Reconfigurable Photosensitivity. *Nano Lett.* **2019**, *19*, 7941–7949. [[CrossRef](#)]
58. White, T.J.; Broer, D.J. Programmable and adaptive mechanics with liquid crystal polymer networks and elastomers. *Nat. Mater.* **2015**, *14*, 1087–1098. [[CrossRef](#)]
59. Nocentini, S.; Parmeggiani, C.; Martella, D.; Wiersma, D.S. Optically Driven Soft Micro Robotics. *Adv. Opt. Mater.* **2018**, *6*, 1800207. [[CrossRef](#)]
60. Ware, T.H.; McConney, M.E.; Wie, J.J.; Tondiglia, V.P.; White, T.J. Voxellated liquid crystal elastomers. *Science* **2015**, *347*, 982–984. [[CrossRef](#)]
61. Yu, Y.; Nakano, M.; Ikeda, T. Directed bending of a polymer film by light. *Nature* **2003**, *425*, 145. [[CrossRef](#)] [[PubMed](#)]
62. Liu, Y.; Xu, B.; Sun, S.; Wei, J.; Wu, L.; Yu, Y. Humidity- and Photo-Induced Mechanical Actuation of Cross-Linked Liquid Crystal Polymers. *Adv. Mater.* **2017**, *29*, 1604792. [[CrossRef](#)] [[PubMed](#)]
63. Xu, W.; Qin, Z.; Chen, C.T.; Kwag, H.R.; Ma, Q.; Sarkar, A.; Buehler, M.J.; Gracias, D.H. Ultrathin thermoresponsive self-folding 3D graphene. *Sci. Adv.* **2017**, *3*, e1701084. [[CrossRef](#)] [[PubMed](#)]
64. Ma, C.; Lu, W.; Yang, X.; He, J.; Le, X.; Wang, L.; Zhang, J.; Serpe, M.J.; Huang, Y.; Chen, T. Bioinspired Anisotropic Hydrogel Actuators with On–Off Switchable and Color-Tunable Fluorescence Behaviors. *Adv. Funct. Mater.* **2018**, *28*, 1704568. [[CrossRef](#)]
65. Cheng, H.; Zhao, F.; Xue, J.; Shi, G.; Jiang, L.; Qu, L. One Single Graphene Oxide Film for Responsive Actuation. *ACS Nano* **2016**, *10*, 9529–9535. [[CrossRef](#)]
66. Wani, O.M.; Zeng, H.; Priimagi, A. A light-driven artificial flytrap. *Nat. Commun.* **2017**, *8*, 1–7. [[CrossRef](#)]
67. Yang, Y.; Zhang, M.; Li, D.; Shen, Y. Graphene-Based Light-Driven Soft Robot with Snake-Inspired Concertina and Serpentine Locomotion. *Adv. Mater. Technol.* **2019**, *4*, 1800366. [[CrossRef](#)]
68. Cheng, Z.; Wang, T.; Li, X.; Zhang, Y.; Yu, H. NIR-Vis-UV Light-Responsive Actuator Films of Polymer-Dispersed Liquid Crystal/Graphene Oxide Nanocomposites. *ACS Appl. Mater. Interfaces* **2015**, *7*, 27494–27501. [[CrossRef](#)]
69. Ma, C.; Le, X.; Tang, X.; He, J.; Xiao, P.; Zheng, J.; Xiao, H.; Lu, W.; Zhang, J.; Huang, Y.; et al. A Multiresponsive Anisotropic Hydrogel with Macroscopic 3D Complex Deformations. *Adv. Funct. Mater.* **2016**, *26*, 8670–8676. [[CrossRef](#)]
70. Hu, Y.; Wu, G.; Lan, T.; Zhao, J.; Liu, Y.; Chen, W. A Graphene-Based Bimorph Structure for Design of High Performance Photoactuators. *Adv. Mater.* **2015**, *27*, 7867–7873. [[CrossRef](#)]

71. Wang, W.; Xiang, C.; Zhu, Q.; Zhong, W.; Li, M.; Yan, K.; Wang, D. Multistimulus Responsive Actuator with GO and Carbon Nanotube/PDMS Bilayer Structure for Flexible and Smart Devices. *ACS Appl. Mater. Interfaces* **2018**, *10*, 27215–27223. [[CrossRef](#)] [[PubMed](#)]
72. Ma, H.; Hou, J.; Wang, X.; Zhang, J.; Yuan, Z.; Xiao, L.; Wei, Y.; Fan, S.; Jiang, K.; Liu, K. Flexible, all-inorganic actuators based on vanadium dioxide and carbon nanotube bimorphs. *Nano Lett.* **2017**, *17*, 421–428. [[CrossRef](#)] [[PubMed](#)]
73. Martella, D.; Nocentini, S.; Nuzhdin, D.; Parmeggiani, C.; Wiersma, D.S. Photonic Microhand with Autonomous Action. *Adv. Mater.* **2017**, *29*, 1704047. [[CrossRef](#)] [[PubMed](#)]
74. Wani, O.M.; Zeng, H.; Wasylczyk, P.; Priimagi, A. Programming Photoresponse in Liquid Crystal Polymer Actuators with Laser Projector. *Adv. Opt. Mater.* **2018**, *6*, 1700949. [[CrossRef](#)]
75. Jiang, Z.; Xu, M.; Li, F.; Yu, Y. Red-light-controllable liquid-crystal soft actuators via low-power excited upconversion based on triplet-triplet annihilation. *J. Am. Chem. Soc.* **2013**, *135*, 16446–16453. [[CrossRef](#)] [[PubMed](#)]
76. Zeng, H.; Wani, O.M.; Wasylczyk, P.; Kaczmarek, R.; Priimagi, A. Self-Regulating Iris Based on Light-Actuated Liquid Crystal Elastomer. *Adv. Mater.* **2017**, *29*, 1701814. [[CrossRef](#)]
77. Van Oosten, C.L.; Bastiaansen, C.W.M.; Broer, D.J. Printed artificial cilia from liquid-crystal network actuators modularly driven by light. *Nat. Mater.* **2009**, *8*, 677–682. [[CrossRef](#)] [[PubMed](#)]
78. Ikeda, T.; Mamiya, J.I.; Yu, Y. Photomechanics of liquid-crystalline elastomers and other polymers. *Angew. Chem. Int. Ed.* **2007**, *46*, 506–528. [[CrossRef](#)]
79. Mol, G.N.; Harris, K.D.; Bastiaansen, C.W.M.; Broer, D.J. Thermo-mechanical responses of liquid-crystal networks with a splayed molecular organization. *Adv. Funct. Mater.* **2005**, *15*, 1155–1159. [[CrossRef](#)]
80. Deng, T.; Yoon, C.; Jin, Q.; Li, M.; Liu, Z.; Gracias, D.H. Self-folding graphene-polymer bilayers. *Appl. Phys. Lett.* **2015**, *106*, 203108. [[CrossRef](#)]
81. Jamal, M.; Zarafshar, A.M.; Gracias, D.H. Differentially photo-crosslinked polymers enable self-assembling microfluidics. *Nat. Commun.* **2011**, *2*, 1–6. [[CrossRef](#)] [[PubMed](#)]
82. Zhao, Q.; Dunlop, J.W.C.; Qiu, X.; Huang, F.; Zhang, Z.; Heyda, J.; Dzubiella, J.; Antonietti, M.; Yuan, J. An instant multi-responsive porous polymer actuator driven by solvent molecule sorption. *Nat. Commun.* **2014**, *5*, 1–8. [[CrossRef](#)] [[PubMed](#)]
83. Cheng, H.; Liu, J.; Zhao, Y.; Hu, C.; Zhang, Z.; Chen, N.; Jiang, L.; Qu, L. Graphene fibers with predetermined deformation as Moisture-triggered actuators and robots. *Angew. Chem. Int. Ed.* **2013**, *52*, 10482–10486. [[CrossRef](#)] [[PubMed](#)]
84. Xiang, C.; Wang, W.; Zhu, Q.; Xue, D.; Zhao, X.; Li, M.; Wang, D. Flexible and Super-Sensitive Moisture-Responsive Actuators by Dispersing Graphene Oxide into Three-Dimensional Structures of Nanofibers and Silver Nanowires. *ACS Appl. Mater. Interfaces* **2020**, *12*, 3245–3253. [[CrossRef](#)] [[PubMed](#)]
85. Dai, M.; Picot, O.T.; Verjans, J.M.N.; De Haan, L.T.; Schenning, A.P.H.J.; Peijs, T.; Bastiaansen, C.W.M. Humidity-responsive bilayer actuators based on a liquid-crystalline polymer network. *ACS Appl. Mater. Interfaces* **2013**, *5*, 4945–4950. [[CrossRef](#)]
86. De Haan, L.T.; Verjans, J.M.N.; Broer, D.J.; Bastiaansen, C.W.M.; Schenning, A.P.H.J. Humidity-responsive liquid crystalline polymer actuators with an asymmetry in the molecular trigger that bend, fold, and curl. *J. Am. Chem. Soc.* **2014**, *136*, 10585–10588. [[CrossRef](#)]
87. Chen, L.; Weng, M.; Zhou, P.; Zhang, L.; Huang, Z.; Zhang, W. Multi-responsive actuators based on a graphene oxide composite: Intelligent robot and bioinspired applications. *Nanoscale* **2017**, *9*, 9825–9833. [[CrossRef](#)]
88. Dawson, C.; Vincent, J.F.V.; Rocca, A.M. How pine cones open. *Nature* **1997**, *390*, 668. [[CrossRef](#)]
89. Harrington, M.J.; Razghandi, K.; Ditsch, F.; Guiducci, L.; Rueggeberg, M.; Dunlop, J.W.C.; Fratzl, P.; Neinhuis, C.; Burgert, I. Origami-like unfolding of hydro-actuated ice plant seed capsules. *Nat. Commun.* **2011**, *2*, 1–7. [[CrossRef](#)]
90. Armon, S.; Efrati, E.; Kupferman, R.; Sharon, E. Geometry and mechanics in the opening of chiral seed pods. *Science* **2011**, *333*, 1726–1730. [[CrossRef](#)]
91. Zhou, Y.; Zhan, P.; Ren, M.; Zheng, G.; Dai, K.; Mi, L.; Liu, C.; Shen, C. Significant stretchability enhancement of a crack-based strain sensor combined with high sensitivity and superior durability for motion monitoring. *ACS Appl. Mater. Interfaces* **2019**, *11*, 7405–7414. [[CrossRef](#)] [[PubMed](#)]

92. Huang, S.; He, G.; Yang, C.; Wu, J.; Guo, C.; Hang, T.; Li, B.; Yang, C.; Liu, D.; Chen, H.J.; et al. Stretchable Strain Vector Sensor Based on Parallely Aligned Vertical Graphene. *ACS Appl. Mater. Interfaces* **2019**, *11*, 1294–1302. [[CrossRef](#)] [[PubMed](#)]
93. Zhou, J.; Xu, X.; Xin, Y.; Lubineau, G. Coaxial Thermoplastic Elastomer-Wrapped Carbon Nanotube Fibers for Deformable and Wearable Strain Sensors. *Adv. Funct. Mater.* **2018**, *28*, 1705591. [[CrossRef](#)]
94. Wan, S.; Zhu, Z.; Yin, K.; Su, S.; Bi, H.; Xu, T.; Zhang, H.; Shi, Z.; He, L.; Sun, L. A Highly Skin-Conformal and Biodegradable Graphene-Based Strain Sensor. *Small Methods* **2018**, *2*, 1700374. [[CrossRef](#)]
95. Shintake, J.; Piskarev, E.; Jeong, S.H.; Floreano, D. Ultrastretchable Strain Sensors Using Carbon Black-Filled Elastomer Composites and Comparison of Capacitive Versus Resistive Sensors. *Adv. Mater. Technol.* **2018**, *3*, 1700284. [[CrossRef](#)]
96. Shi, G.; Zhao, Z.; Pai, J.H.; Lee, I.; Zhang, L.; Stevenson, C.; Ishara, K.; Zhang, R.; Zhu, H.; Ma, J. Highly Sensitive, Wearable, Durable Strain Sensors and Stretchable Conductors Using Graphene/Silicon Rubber Composites. *Adv. Funct. Mater.* **2016**, *26*, 7614–7625. [[CrossRef](#)]
97. Cheng, Y.; Wang, R.; Sun, J.; Gao, L. A Stretchable and Highly Sensitive Graphene-Based Fiber for Sensing Tensile Strain, Bending, and Torsion. *Adv. Mater.* **2015**, *27*, 7365–7371. [[CrossRef](#)]
98. Amjadi, M.; Turan, M.; Clementson, C.P.; Sitti, M. Parallel Microcracks-based Ultrasensitive and Highly Stretchable Strain Sensors. *ACS Appl. Mater. Interfaces* **2016**, *8*, 5618–5626. [[CrossRef](#)]
99. Choi, D.Y.; Kim, M.H.; Oh, Y.S.; Jung, S.H.; Jung, J.H.; Sung, H.J.; Lee, H.W.; Lee, H.M. Highly stretchable, hysteresis-free ionic liquid-based strain sensor for precise human motion monitoring. *ACS Appl. Mater. Interfaces* **2017**, *9*, 1770–1780. [[CrossRef](#)]
100. Li, Y.; Zhou, B.; Zheng, G.; Liu, X.; Li, T.; Yan, C.; Cheng, C.; Dai, K.; Liu, C.; Shen, C.; et al. Continuously prepared highly conductive and stretchable SWNT/MWNT synergistically composited electrospun thermoplastic polyurethane yarns for wearable sensing. *J. Mater. Chem. C* **2018**, *6*, 2258–2269. [[CrossRef](#)]
101. Xing, W.; Hu, J.; Kung, S.C.; Donavan, K.C.; Yan, W.; Wu, R.; Penner, R.M. A chemically-responsive nanojunction within a silver nanowire. *Nano Lett.* **2012**, *12*, 1729–1735. [[CrossRef](#)] [[PubMed](#)]
102. Lopez-Sanchez, O.; Lembke, D.; Kayci, M.; Radenovic, A.; Kis, A. Ultrasensitive photodetectors based on monolayer MoS<sub>2</sub>. *Nat. Nanotechnol.* **2013**, *8*, 497–501. [[CrossRef](#)] [[PubMed](#)]
103. Kim, J.S.; Yoo, H.W.; Choi, H.O.; Jung, H.T. Tunable volatile organic compounds sensor by using thiolated ligand conjugation on MoS<sub>2</sub>. *Nano Lett.* **2014**, *14*, 5941–5947. [[CrossRef](#)] [[PubMed](#)]
104. Kumar, R.; Goel, N.; Kumar, M. UV-Activated MoS<sub>2</sub> Based Fast and Reversible NO<sub>2</sub> Sensor at Room Temperature. *ACS Sens.* **2017**, *2*, 1744–1752. [[CrossRef](#)]
105. Park, M.; Park, Y.J.; Chen, X.; Park, Y.K.; Kim, M.S.; Ahn, J.H. MoS<sub>2</sub>-Based Tactile Sensor for Electronic Skin Applications. *Adv. Mater.* **2016**, *28*, 2556–2562. [[CrossRef](#)]

**Publisher’s Note:** MDPI stays neutral with regard to jurisdictional claims in published maps and institutional affiliations.



© 2020 by the authors. Licensee MDPI, Basel, Switzerland. This article is an open access article distributed under the terms and conditions of the Creative Commons Attribution (CC BY) license (<http://creativecommons.org/licenses/by/4.0/>).